Journal of Systems Engineering and Electronics
Vol. 35, No. 3, June 2024, pp.732 – 740

A dual adaptive unscented Kalman filter algorithm for SINS-based integrated navigation system

LYU Xu[1], MENG Ziyang[1], LI Chunyu[1], CAI Zhenyu[2,*], HUANG Yi[3], LI Xiaoyong[3], and YU Xingkai[4]

1. Department of Precision Instrument, Tsinghua University, Beijing 100084, China; 2. College of Mechanical and Power Engineering, Three Gorges University, Yichang 443002, China; 3. Unit 91001 of the PLA, Beijing 100161, China; 4. School of Control and Computer Engineering, North China Electric Power University, Beijing 100096, China

Abstract: In this study, the problem of measuring noise pollution distribution by the intertial-based integrated navigation system is effectively suppressed. Based on nonlinear inertial navigation error modeling, a nested dual Kalman filter framework structure is developed. It consists of unscented Kalman filter (UKF) master filter and Kalman filter slave filter. This method uses nonlinear UKF for integrated navigation state estimation. At the same time, the exact noise measurement covariance is estimated by the Kalman filter dependency filter. The algorithm based on dual adaptive UKF (Dual-AUKF) has high accuracy and robustness, especially in the case of measurement information interference. Finally, vehicle-mounted and ship-mounted integrated navigation tests are conducted. Compared with traditional UKF and the Sage-Husa adaptive UKF (SH-AUKF), this method has comparable filtering accuracy and better filtering stability. The effectiveness of the proposed algorithm is verified.

Keywords: Kalman filter, dual-adaptive, integrated navigation, unscented Kalman filter (UKF), robust.

DOI: 10.23919/JSEE.2024.000060

1. Introduction

The integrated navigation system uses information fusion technology to combine various navigation systems. Higher navigation accuracy than any single system can be achieved [1,2]. Attitude, speed, and position are the keys to vehicle navigation information, which determine the vehicle precise arrival at the predetermined location [3,4]. Strapdown inertial navigation system (SINS)/global positioning system (GPS) or SINS/Doppler velocity log (DVL) can be assembled to provide definitive guidance information [5]. The two have complementary advantages and combination of both is an effective means to achieve high-precision and high-reliability navigation.

It is well known that Kalman filter is an effective means of integrated navigation information fusion when the system is linear. Unfortunately, navigation systems in real applications are not always nonlinear. Some nonlinear filters such as extended Kalman filter (EKF) and unscented Kalman filter (UKF) have been developed [6,7]. And if there are severe nonlinearities for the navigation system, EKF is very difficult to tune and always give inaccurate and unreliable state estimates [8]. Consequently, the interference of time-varying noise on the system was reduced through innovative statistical adaptive adjustment of system noise and measurement noise in [9]. However, systems that use Taylor's formula expansion approximation will introduce some errors and degrade the accuracy. Nevertheless, UKF has a more significant performance over EKF. The UKF with unsecond transformation (UT) propagation can accurately capture the mean and covariance of system [10–12]. As a result, this paper will investigate the problem based on UKF.

As we all know, the integrated navigation system achieves optimal state estimation by determining some prior information [13]. The SINS is a highly autonomous device. Therefore, the process noise covariance matrix $\boldsymbol{Q}_k$ is relatively stable. However, because the external environment is complex, the measurement error caused is difficult to estimate [14,15]. As a result, the initial measurement noise matrix $\boldsymbol{R}_k$ is inconsistent with the changing reality, and errors are accumulated or even the filtering divergence [16]. To address the non-Gaussian phenomenon of noise $\boldsymbol{R}_k$, the following typical methods are proposed. In 2018, Xu et al. researched the applications of SINS/ultra short baseline (USBL) integrated navigation system based adaptive Kalman filter (AKF) [17]. In 2021, Hou et al. proposed an improved AKF for SINS/DVL integrated navigation [18]. There are four cate-

Manuscript received December 14, 2023.
*Corresponding author.
This work was supported by China Postdoctoral Science Foundation (2023M741882) and the National Natural Science Foundation of China (62103222; 62273195).

gories of AKF which are Bayesian, maximum likelihood, correlation and covariance matching. The Sage-Husa AKF (SH-AKF) as a covariance matching estimation strategy is proposed and has been widely utilized. In recent years, Meng et al. proposed a Sage-Husa adaptive UKF (SH-AUKF) for the direct filtering in SINS/global navigation satellite system (GNSS) integration navigation [19]. In a word, AKF can effectively overcome the shortcomings of inconsistent real-world variable noise. The robustness and accuracy of integrated navigation systems can be improved.

However, there are also many shortcomings and its limitations in practical application for the AKF. As is known, the classical SH-AKF is a recursive algorithm in essence, which estimates the noise matrix of the next moment according to the noise matrix of the previous moment. Therefore, the errors will inevitably accumulate in the process of recursion, which will eventually have a negative influence on the accuracy and stability of system. In addition, when the measurement information is poor or almost missing, the estimation of the noise matrix at the next moment is greatly affected. And it is likely to cause a large error of the noise matrix which even leads to the filtering divergence. Furthermore, the performance of AKF is greatly dependent on the initial measurement noise matrix, which is also difficult to be determined.

Therefore, this paper mainly refers to the advantages of dual Kalman filters to solve the above problems. Astroza et al. and Song et al. studied dual adaptive Kalman filters for nonlinear finite element model updating [20,21]. In 2019, Guo et al. used double Kalman to estimate the state of charge and parameters of lithium-ion batteries [22]. Li et al. studied a regularization-based dual AKF for identifying sudden structural damage [23]. Obviously, the structural design of double Kalman filter has significant advantages in system stability.

Based on the above analysis, a combined navigation algorithm based on dual adaptive UKF is proposed in this paper. This method improves the accuracy and robustness of the integrated navigation system. Dual adaptive filters employ correlation filters to update the measurement noise matrix. Two real sensor data from SINS/GPS and SINS/DVL are used to estimate the navigation performance using dual adaptive UKF (Dual-AUKF), UKF and SH-AUKF. This paper introduces dual AKFs into the field of integrated navigation for the first time, which is a research worthy of wide application. The work of dual AKFs will broaden the research horizons of inertial integrated navigation and is verified in this paper.

This paper is organized as follows. Section 2 covers the construction of the SINS nonlinear error model. Section 3 presents the derivation of the improved filtering algorithm. Section 4 discusses field testing and analysis. Finally, concluding remarks are given in Section 5.

2. SINS nonlinear error model construction

The error differential equation of strapdown inertial navigation is derived from the basic strapdown inertial navigation equation. The error differential error equation consists of attitude error part, velocity error part, and position error part.

Denote the misalignment angle error as $\boldsymbol{\alpha} = [\alpha_x,\ \alpha_y,\ \alpha_z]^{\mathrm{T}}$, which are pitch error, roll error and yaw error respectively. Denote velocity error as $\delta\boldsymbol{v}^n = \tilde{\boldsymbol{v}}^n - \boldsymbol{v}^n$ with $\delta\boldsymbol{v}^n = [\delta v_E^n, \delta v_N^n, \delta v_U^n]^{\mathrm{T}}$ defined in the East-North-Up frame. $\delta\boldsymbol{p} = [\delta L,\ \delta\lambda,\ \delta h]^{\mathrm{T}}$ is denoted as position error, which are latitude error, longitude error and height error, respectively. With (1)−(5), the nonlinear error model based on Euler angles are given by

$$\begin{cases} \dot{\boldsymbol{\alpha}} = \boldsymbol{C}_{\omega}^{-1}\left[\left(\boldsymbol{I}_{3\times3} - \boldsymbol{C}_{n}^{n'}\right)\tilde{\boldsymbol{\omega}}_{in}^{n} + C_{n}^{n'}\delta\boldsymbol{\omega}_{in}^{n} - \boldsymbol{C}_{b}^{n'}\delta\boldsymbol{\omega}_{ib}^{b}\right] \\ \delta\dot{v}^n = (\boldsymbol{I}_{3\times3} - \boldsymbol{C}_{n'}^{n})\boldsymbol{C}_{b}^{n'}\tilde{\boldsymbol{f}}_{ib}^{b} + \boldsymbol{C}_{n'}^{n}\boldsymbol{C}_{b}^{n'}\delta\boldsymbol{f}_{ib}^{b} - \\ \quad (2\delta\boldsymbol{\omega}_{ie}^{n} + \delta\boldsymbol{\omega}_{en}^{n})\times\tilde{\boldsymbol{v}}^n - (2\tilde{\boldsymbol{\omega}}_{ie}^{n} + \tilde{\boldsymbol{\omega}}_{en}^{n})\times\delta\boldsymbol{v}^n \\ \delta\dot{\boldsymbol{p}} = \boldsymbol{M}_{pv}\delta\boldsymbol{v}^n + \boldsymbol{M}_{pp}\delta\boldsymbol{p} \end{cases} \tag{1}$$

where

$$\boldsymbol{C}_{n'}^{n} = \begin{bmatrix} c\alpha_y c\alpha_z - s\alpha_x s\alpha_y s\alpha_z & -c\alpha_x s\alpha_z & s\alpha_y c\alpha_z + c\alpha_y s\alpha_x s\alpha_z \\ c\alpha_y s\alpha_z + c\alpha_z s\alpha_x s\alpha_y & c\alpha_x c\alpha_z & s\alpha_y s\alpha_z - c\alpha_y s\alpha_x c\alpha_z \\ -c\alpha_x s\alpha_y & s\alpha_x & c\alpha_x c\alpha_y \end{bmatrix}, \tag{2}$$

$$\boldsymbol{C}_{\omega}^{-1} = \frac{1}{c\alpha_x}\begin{bmatrix} c\alpha_x c\alpha_y & 0 & c\alpha_x s\alpha_y \\ s\alpha_x s\alpha_y & c\alpha_x & -s\alpha_x c\alpha_y \\ -s\alpha_y & 0 & c\alpha_y \end{bmatrix}, \tag{3}$$

$$\boldsymbol{M}_{pv} = \begin{bmatrix} 0 & 1/\left(\tilde{R}_M + \tilde{h}\right) & 0 \\ \sec\tilde{L}/\left(\tilde{R}_N + \tilde{h}\right) & 0 & 0 \\ 0 & 0 & 1 \end{bmatrix}, \tag{4}$$

$$\boldsymbol{M}_{pp} = \begin{bmatrix} 0 & 0 & 0 \\ \dfrac{\tilde{v}_e^n \sec\tilde{L}\tan\tilde{L}}{\tilde{R}_N + \tilde{h}} & 0 & 0 \\ 0 & 0 & 0 \end{bmatrix}, \tag{5}$$

the symbol c represents the cosine function and s represents the sine function. $\delta\boldsymbol{f}_{ib}^{b}$ is approximately equal to the accelerometer device error ∇^b. $\boldsymbol{I}_3$ is the 3×3 unit matrix. $\tilde{\boldsymbol{\omega}}_{ie}^{n}$ is the earth rotation rate in navigation frame and $\tilde{\boldsymbol{\omega}}_{en}^{n}$ is a function of velocity and position with $\tilde{\boldsymbol{\omega}}_{in}^{n} = \tilde{\boldsymbol{\omega}}_{ie}^{n} + \tilde{\boldsymbol{\omega}}_{en}^{n}$. $\delta\boldsymbol{\omega}_{ie}^{n}$ and $\delta\boldsymbol{\omega}_{en}^{n}$ are the calculation parameter errors, which are respectively given by

$$\delta\boldsymbol{\omega}_{ie}^{n}=\begin{bmatrix}0\\-\omega_{ie}\sin\tilde{L}\cdot\delta L\\ \omega_{ie}\cos\tilde{L}\cdot\delta L\end{bmatrix},\tag{6}$$

$$\delta\boldsymbol{\omega}_{en}^{n}=\begin{bmatrix}-\delta v_{N}^{n}/\left(R_{M}+\tilde{h}\right)\\ \delta\dot{\lambda}\cos\tilde{L}-\dot{\tilde{\lambda}}\sin\tilde{L}\cdot\delta L\\ \delta\dot{\lambda}\sin\tilde{L}+\dot{\tilde{\lambda}}\cos\tilde{L}\cdot\delta L\end{bmatrix}.\tag{7}$$

3. Improved filtering algorithm derivation

In this paper, the state space model of the stochastic system could be decomposed likewise

$$\begin{cases}\boldsymbol{x}_k=f(\boldsymbol{x}_{k-1})+\boldsymbol{\omega}_{k-1}\\ \boldsymbol{y}_k=h(\boldsymbol{x}_k)+\boldsymbol{r}_k\end{cases}\tag{8}$$

where $\boldsymbol{x}_k\in\mathbf{R}^n$ is the n-dimensional state vector at time k, which is necessary to estimate. $\boldsymbol{y}_k\in\mathbf{R}^m$ is the m-dimensional measurement vector which can be measured toward period example. $f(\cdot)$ is the dynamic model and $h(\cdot)$ is the measurement model. $\boldsymbol{\omega}_{k-1}$ is the process noise with zero mean and covariance $\boldsymbol{Q}_{k-1}$. $\boldsymbol{r}_k$ is the measurement noise with zero mean and covariance $\boldsymbol{R}_k$.

3.1 SH-AKF based UKF

In this subsection, we will firstly review UKF, which is proposed to overcome the aforementioned challenges in using EKF for estimation of nonlinear state-space models [24]. UKF is based on the UT, which is a statistical linearization method which uses deterministic Sigma points. The basic UKF process of calculation is shown as follows.

Algorithm 1 UKF

Time propagation:

$$\boldsymbol{\chi}_{i,k/k-1}=\boldsymbol{f}(\boldsymbol{\chi}_{i,k-1})$$

$$\hat{\boldsymbol{x}}_{k/k-1}=\sum_{i=0}^{2n}W_i^m\boldsymbol{\chi}_{i,k/k-1},\ \ i=0,1,\cdots,2n$$

$$\boldsymbol{P}_{xx,k/k-1}=\sum_{i=0}^{2n}W_i^c(\boldsymbol{\chi}_{i,k/k-1}-\hat{\boldsymbol{x}}_{k/k-1})(\boldsymbol{\chi}_{i,k/k-1}-\hat{\boldsymbol{x}}_{k/k-1})^{\mathrm{T}}+\boldsymbol{Q}_{k-1}$$

where $\boldsymbol{\chi}_{i,k/k-1}$ is the sigma point and W_i^m, W_i^c are the weights.

Update:

$$\boldsymbol{\chi}_{k/k-1}^{*}=[\hat{\boldsymbol{x}}_{k/k-1},\hat{\boldsymbol{x}}_{k/k-1}+\sqrt{(n+\lambda)\boldsymbol{P}_{xx,k/k-1}},\ \hat{\boldsymbol{x}}_{k/k-1}-\sqrt{(n+\lambda)\boldsymbol{P}_{xx,k/k-1}}]$$

$$\boldsymbol{\eta}_{i,k/k-1}=\boldsymbol{h}\left(\boldsymbol{\chi}_{i,k/k-1}^{*}\right)$$

$$\hat{\boldsymbol{y}}_{k/k-1}=\sum_{i=0}^{2n}W_i^m\boldsymbol{\eta}_{i,k/k-1}$$

$$\boldsymbol{P}_{yy,k/k-1}=\sum_{i=0}^{2n}W_i^c(\boldsymbol{\eta}_{i,k/k-1}-\hat{\boldsymbol{y}}_{k/k-1})(\boldsymbol{\eta}_{i,k/k-1}-\hat{\boldsymbol{y}}_{k/k-1})^{\mathrm{T}}+\boldsymbol{R}_k$$

$$\boldsymbol{P}_{xy,k/k-1}=\sum_{i=0}^{2n}W_i^c\left(\boldsymbol{\chi}_{i,k/k-1}^{*}-\hat{\boldsymbol{x}}_{k/k-1}\right)(\boldsymbol{\eta}_{i,k/k-1}-\hat{\boldsymbol{x}}_{k/k-1})^{\mathrm{T}}$$

$$\boldsymbol{K}_k=\boldsymbol{P}_{xy,k/k-1}\boldsymbol{P}_{yy,k/k-1}^{-1}$$

$$\hat{\boldsymbol{x}}_k=\hat{\boldsymbol{x}}_{k/k-1}+\boldsymbol{K}_k(\boldsymbol{y}_k-\hat{\boldsymbol{y}}_{k/k-1})$$

$$\boldsymbol{P}_k=\boldsymbol{P}_{xx,k/k-1}-\boldsymbol{K}_k\boldsymbol{P}_{yy,k/k-1}\boldsymbol{K}_k^{\mathrm{T}}$$

As we know, the aim of the adaptive filter is to estimate the joint posterior distribution of the states and noise covariance. The classical Kalman filter or nonlinear filters can work if the noise covariance matrix $\boldsymbol{R}_k$ is known. However, if the matrix $\boldsymbol{R}_k$ is unknow or time-varying distributed by complex external environment, the classical filter is difficult to have an accurate performance. Hence, the adaptive filter is necessary to study, which is obtained as follows.

Algorithm 2 SH-AUKF

Time propagation:

$$\boldsymbol{\chi}_{i,k/k-1}=\boldsymbol{f}(\boldsymbol{\chi}_{i,k-1})$$

$$\hat{\boldsymbol{x}}_{k/k-1}=\sum_{i=0}^{2n}W_i^m\boldsymbol{\chi}_{i,k/k-1},\ \ i=0,1,\cdots,2n$$

$$\boldsymbol{P}_{xx,k/k-1}=\sum_{i=0}^{2n}W_i^c(\boldsymbol{\chi}_{i,k/k-1}-\hat{\boldsymbol{x}}_{k/k-1})(\boldsymbol{\chi}_{i,k/k-1}-\hat{\boldsymbol{x}}_{k/k-1})^{\mathrm{T}}+\boldsymbol{Q}_{k-1}$$

Update:

$$\boldsymbol{\chi}_{k/k-1}^{*}=[\hat{\boldsymbol{x}}_{k/k-1},\hat{\boldsymbol{x}}_{k/k-1}+\sqrt{(n+\lambda)\boldsymbol{P}_{xx,k/k-1}},\ \hat{\boldsymbol{x}}_{k/k-1}-\sqrt{(n+\lambda)\boldsymbol{P}_{xx,k/k-1}}]$$

$$\boldsymbol{\eta}_{i,k/k-1}=\boldsymbol{h}\left(\boldsymbol{\chi}_{i,k/k-1}^{*}\right)$$

$$\hat{\boldsymbol{y}}_{k/k-1}=\sum_{i=0}^{2n}W_i^m\boldsymbol{\eta}_{i,k/k-1}$$

$$\boldsymbol{v}_k=\boldsymbol{y}_k-\boldsymbol{H}_k\hat{\boldsymbol{x}}_{k/k-1}$$

$$\boldsymbol{R}_k=(1-d_k)\boldsymbol{R}_{k-1}+d_k\left(\boldsymbol{v}_k\boldsymbol{v}_k^{\mathrm{T}}-\boldsymbol{H}_k\boldsymbol{P}_{xx,k/k-1}\boldsymbol{H}_k^{\mathrm{T}}\right)$$

$$d_k=(1-b)/\left(1-b^{k+1}\right)$$

where b is the forgetting factor and $b\in(0.95\sim0.99)$. Then $\boldsymbol{P}_{xy,k/k-1}$, $\boldsymbol{P}_{yy,k/k-1}$, $\boldsymbol{K}_k$, $\hat{\boldsymbol{x}}_k$ and $\boldsymbol{P}_k$ are obtained as UKF.

3.2 Dual-AKF based integrated navigation

In Subsection 3.1, we derive UKF and SH-AUKF, which can solve linear or nonlinear integrated navigation system problems with time-varying measurement noise covariance. However, there are some defects for the SH-AUKF which is difficult to obtain the accurate measurement noise covariance matrix.

Firstly, the classical SH-AUKF is essentially a recursive algorithm. The measurement noise covariance matrix of the next period is obtained based on the measurement noise covariance matrix of the previous period. However, the errors generated by the recursion gradually accumulate, and the accuracy and stability of the integrated navigation system are negatively affected. Secondly, the estimation accuracy of the next period measurement noise matrix greatly depends on the accuracy of the previous measurement noise matrix. Therefore, both sudden changes in measurement information and time-varying non-Gaussian distribution of measurement noise will cause inaccurate estimation of the next measurement noise matrix. In addition, the SH-AUKF algorithm is very dependent on the initial measurement noise matrix. Unfortunately, accurate initial values are very difficult to obtain. In summary, especially in the case of poor measurements, the performance of SH-AUKF will be greatly limited. Therefore, a combined navigation based on dual adaptive unscented Kalman filters is proposed to overcome the above shortcomings, as shown in Fig. 1.

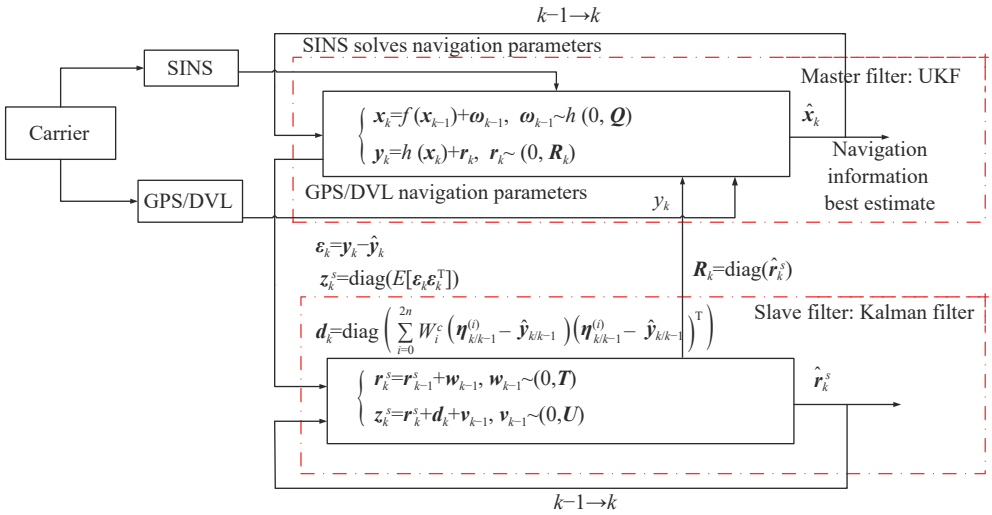

Fig. 1 Flow chart of Dual-AUKF

The Dual-AUKF algorithm structure consists of UKF master filter and Kalman filter slave filter. This method applies the UKF algorithm to SINS/GPS or SINS/DVL integrated navigation. A built-in nested Kalman filter estimation structure is designed to accurately estimate observation noise $\boldsymbol{R}_k$ in this method. For the main filter, UKF is used to obtain the optimal estimate of the nonlinear error model. For dependent filters, the diagonal terms of $\boldsymbol{R}_k$ is treated as unknown parameters. This parameter is considered as the state of the slave filter to be accurately estimated.

In the part of time propagation for master filter, $\boldsymbol{z}_k=\mathrm{diag}(E[\boldsymbol{v}_k\boldsymbol{v}_k^{\mathrm{T}}])$ is obtained as the measurement of Kalman filter, which is gained from the innovation $\boldsymbol{v}_k$. And $\boldsymbol{z}_{k/k-1}^r=\hat{\boldsymbol{r}}_{k/k-1}+\mathrm{diag}(l_k)$ is obtained as one-step state prediction of slave filter in the part of time propagation for slave filter. Then the posterior estimate of the mean and the posterior estimate of the covariance matrix of $\boldsymbol{R}_k$ is obtained in the part of update for slave filter. In addition, in this part, the accurate measurement noise covariance matrix embedded in master filter is also estimated by $\hat{\boldsymbol{R}}_k=\mathrm{diag}(\hat{\boldsymbol{r}}_k)$. Finally, in the part of update for master filter, the posterior mean and the posterior covariance matrix are updated for the master filter of UKF with the accurately estimated $\hat{\boldsymbol{R}}_k$ obtained by the slave filter of Kalman filter. It is noted that the process noise covariance matrix $\boldsymbol{T}$ and measurement noise covariance matrix $\boldsymbol{U}$ for the slave filter of Kalman filter are time-invariant matrix, which have an important impact on the performance of slave filter. Therefore, it is extremely necessary to have an approximate determination for $\boldsymbol{T}$ and $\boldsymbol{U}$. The Dual-AUKF algorithm is described and overviewed in Algorithm 3.

Algorithm 3 Dual-AUKF

Time propagation for master filter:

$$\boldsymbol{\chi}_{i,k/k-1}=\boldsymbol{f}(\boldsymbol{\chi}_{i,k-1})$$

$$\hat{\boldsymbol{x}}_{k/k-1}=\sum_{i=0}^{2n}W_i^m\boldsymbol{\chi}_{i,k/k-1},\ \ i=0,1,\cdots,2n$$

$$\boldsymbol{P}_{xx,k/k-1}=\sum_{i=0}^{2n}W_i^c(\boldsymbol{\chi}_{i,k/k-1}-\hat{\boldsymbol{x}}_{k/k-1})(\boldsymbol{\chi}_{i,k/k-1}-\hat{\boldsymbol{x}}_{k/k-1})^{\mathrm{T}}+\boldsymbol{Q}_{k-1}$$

$$\boldsymbol{\chi}^*_{k/k-1}=[\hat{\boldsymbol{x}}_{k/k-1},\hat{\boldsymbol{x}}_{k/k-1}+\sqrt{(n+\lambda)\boldsymbol{P}_{xx,k/k-1}},\ \hat{\boldsymbol{x}}_{k/k-1}-\sqrt{(n+\lambda)\boldsymbol{P}_{xx,k/k-1}}]$$

$$\boldsymbol{\eta}_{i,k/k-1}=\boldsymbol{h}\left(\boldsymbol{\chi}^*_{i,k/k-1}\right)$$

$$\hat{\boldsymbol{y}}_{k/k-1}=\sum_{i=0}^{2n}W_i^m\boldsymbol{\eta}_{i,k/k-1}$$

$$\boldsymbol{v}_k=\boldsymbol{y}_k-\boldsymbol{H}_k\hat{\boldsymbol{x}}_{k/k-1}$$

$$\boldsymbol{z}_k=\mathrm{diag}(E[\boldsymbol{v}_k\boldsymbol{v}_k{}^{\mathrm{T}}])$$

Time propagation for slave filter:

$$\boldsymbol{r}_{k/k-1}=\boldsymbol{r}_{k-1}$$

$$\boldsymbol{P}_{rr,k/k-1}=\boldsymbol{P}_{rr,k-1}+\boldsymbol{T}$$

$$\boldsymbol{z}^r_{k/k-1}=\hat{\boldsymbol{r}}_{k/k-1}+\mathrm{diag}\,(l_k)$$

$$l_k=\sum_{i=0}^{2n}W_i^c(\boldsymbol{\eta}_{i,k/k-1}-\hat{\boldsymbol{y}}_{k/k-1})(\boldsymbol{\eta}_{i,k/k-1}-\hat{\boldsymbol{y}}_{k/k-1})^{\mathrm{T}}$$

Update for slave filter:

$$\boldsymbol{P}_{zz,k/k-1}=\boldsymbol{P}_{rr,k-1}+\boldsymbol{U}$$

$$\boldsymbol{P}_{rz,k/k-1}=\boldsymbol{P}_{rr,k/k-1}$$

$$\hat{\boldsymbol{r}}_k=\hat{\boldsymbol{r}}_{k/k-1}+\boldsymbol{K}^r_k\left(\boldsymbol{z}^r_k-\boldsymbol{z}^r_{k/k-1}\right)$$

$$\boldsymbol{P}_{rr,k}=\boldsymbol{P}_{rr,k/k-1}-\boldsymbol{K}^r_k\boldsymbol{P}_{zz,k/k-1}(\boldsymbol{K}^r_k)^{\mathrm{T}}$$

$$\hat{\boldsymbol{R}}_k=\mathrm{diag}(\hat{\boldsymbol{r}}_k)$$

Update for master filter:

$$\boldsymbol{P}_{yy,k/k-1}=\sum_{i=0}^{2n}W_i^c(\boldsymbol{\eta}_{i,k/k-1}-\hat{\boldsymbol{y}}_{k/k-1})(\boldsymbol{\eta}_{i,k/k-1}-\hat{\boldsymbol{y}}_{k/k-1})^{\mathrm{T}}+\hat{\boldsymbol{R}}_k$$

$$\boldsymbol{P}_{xy,k/k-1}=\sum_{i=0}^{2n}W_i^c\left(\boldsymbol{\chi}^*_{i,k/k-1}-\hat{\boldsymbol{x}}_{k/k-1}\right)(\boldsymbol{\eta}_{i,k/k-1}-\hat{\boldsymbol{x}}_{k/k-1})^{\mathrm{T}}$$

$$\boldsymbol{K}_k=\boldsymbol{P}_{xy,k/k-1}\boldsymbol{P}^{-1}_{yy,k/k-1}$$

$$\hat{\boldsymbol{x}}_k=\hat{\boldsymbol{x}}_{k/k-1}+\boldsymbol{K}_k(\boldsymbol{y}_k-\hat{\boldsymbol{y}}_{k/k-1})$$

$$\boldsymbol{P}_k=\boldsymbol{P}_{xx,k/k-1}-\boldsymbol{K}_k\boldsymbol{P}_{yy,k/k-1}\boldsymbol{K}^{\mathrm{T}}_k$$

4. Field test and analysis

In this section, the vehicle-mounted SINS/GPS and ship-mounted SINS/DVL integrated navigation systems are tested. Based on dual adaptive filters, Sage-Husa adaptive filter, classical Kalman filter performance is evaluated in this paper. They are denoted as Dual-AUKF, SH-AUKF and UKF respectively. Then the state vectors are expressed as follows:

$$\boldsymbol{x}=\left[\boldsymbol{\alpha}^{\mathrm{T}},(\delta\boldsymbol{v}^n)^{\mathrm{T}},\delta\boldsymbol{p}^{\mathrm{T}},(\boldsymbol{\varepsilon}^b)^{\mathrm{T}},\nabla^b\right]^{\mathrm{T}}\tag{9}$$

where $\boldsymbol{\varepsilon}^b$ denotes the gyroscope drift and ∇^b denotes the accelerometer drift bias. Velocity and position errors are defined as SINS/GPS observations. Velocity is defined as the observed value of SINS/DVL. Two observation matrices are given by

$$\boldsymbol{H}_{\mathrm{sins/gps}}=\begin{bmatrix}\boldsymbol{0}_{3\times3}&\boldsymbol{I}_{3\times3}&\boldsymbol{0}_{3\times3}&\boldsymbol{0}_{3\times6}\\ \boldsymbol{0}_{3\times3}&\boldsymbol{0}_{3\times3}&\boldsymbol{I}_{3\times3}&\boldsymbol{0}_{3\times6}\end{bmatrix},\tag{10}$$

$$\boldsymbol{H}_{\mathrm{sins/dvl}}=\begin{bmatrix}(-\tilde{\boldsymbol{v}}_n)\times&\boldsymbol{I}_{3\times3}&\boldsymbol{0}_{3\times3}&\boldsymbol{0}_{3\times6}\end{bmatrix}.\tag{11}$$

4.1 Car-mounted experiment

In this section, the superior performance of the algorithm is illustrated in on-vehicle experiments. Low-precision SINS (STIM300) and GPS antennas are installed in the experimental vehicle. In addition, a high-precision optical fiber SINS is installed on the experimental vehicle and serves as a reference system. The test trajectory is shown in Fig. 2. The experiment lasts about 3 000 s and is conducted on an open road with good GPS signals.

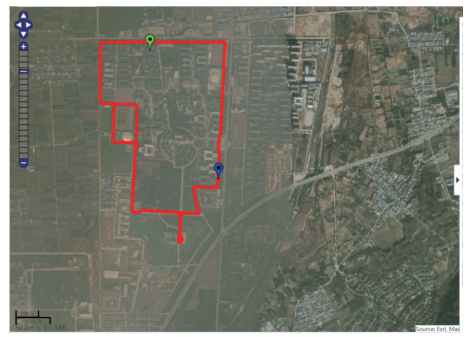

Fig. 2 Trajectory of the car

In the experiments, the attitude and position accuracy are compared. The SH-AUKF algorithm and the Dual-AUKF algorithm are two adaptive Kalman algorithms used to deal with parameter estimation problems when the noise statistics are unknown or time-varying. To com-

pare the performance of these methods, the velocity and position provided by GPS are added with 1 m/s and 10 m errors respectively, while the noise is zero-mean white noise. In addition, the initial attitude error is set: the horizontal error is 1° and the yaw error is 3°. The specifications of STIM300S are shown in Table 1.

Table 1 Specifications of STIM300

Quantity	Gyro	Accelerometer
Dynamic range	±400°/s	±10g
Bias	⩽0.5°/h	⩽0.05 mg
Update rate	125 Hz	125 Hz

Three methods of UKF, SH-AUKF and Dual-AUKF are used to realize SINS/GPS integrated navigation. The estimate error results of attitude and position errors are shown in Fig. 3.

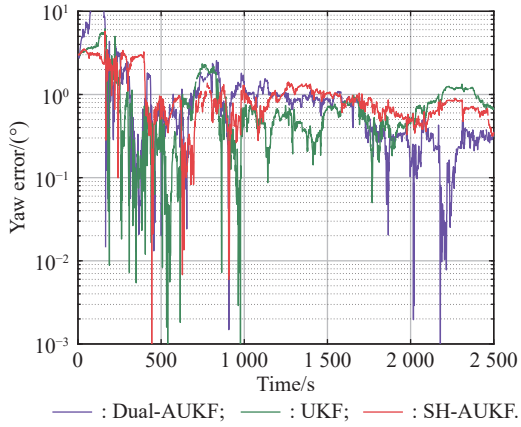

Fig. 3 Yaw estimate errors

We know that the difference between pitch error and roll error is negligible, and their convergence speed and filtering accuracy are quite equal. The main reason is that the car-mounted experiment is carried out on a relative flat field. However, as shown in Fig. 3, the performance of three methods is distinguished from the yaw error. Dual-AUKF has a better performance than SH-AUKF and UKF, especially after 1 000 s. In addition, SH-AUKF and UKF have a tendency to diverge after 2 000 s and the yaw error of UKF is more than 1° from 2 200 s to 2 400 s.

The position error is shown in Fig. 4 and Fig. 5. It can be seen that the latitude and longitude position errors of Dual-AUKF are more stable and smaller than those of SH-AUKF and UKF. At the same time, the corresponding speed error is also reduced accordingly.

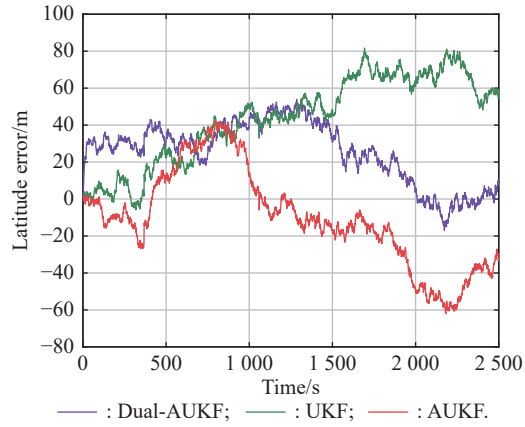

Fig. 4 Latitude estimate errors

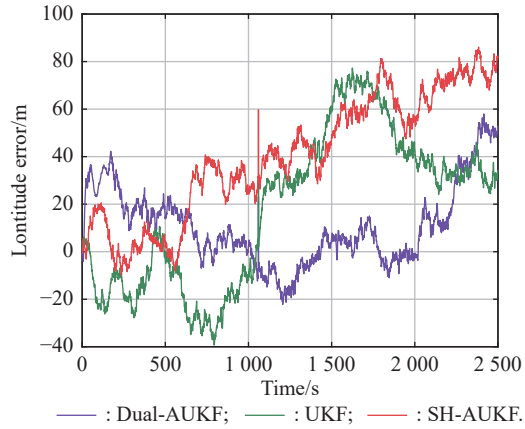

Fig. 5 Longitude estimate errors

In addition, the average error value of the three SINS/GPS methods are shown in Table 2. Compared with SH-AUKF, the attitude of this new Dual-AUKF is reduced by 3.2%, 5.1%, and 11.1% respectively. For vehicle integrated navigation, the Dual-AUKF algorithm has smaller heading angle error and position error. Dual-AUKF is more robust and stable than SH-AUKF and UKF. It is concluded that Dual-AUKF outperforms SH-AUKF and UKF in both navigation accuracy and stability in the integrated navigation of SINS/GPS.

Table 2 Mean of state errors

Average estimation error	UKF	SH-AUKF	Dual-AUKF
Pitch error/(°)	0.2835	0.2682	0.2596
Roll error/(°)	0.3940	0.3965	0.3762
Yaw error/(°)	1.2798	1.2079	1.0744
East velocity error/(m·s^{-1})	0.0207	0.0312	0.0034
North velocity error/(m·s^{-1})	0.0323	0.0078	−0.0221
Latitude error/m	33.0567	−5.6838	−35.8853
Latigude error/m	37.8510	42.4647	−5.3834

4.2 Shipboard test

In order to further assess the benefits and drawbacks of the proposed method, a ship-mounted experiment is carried out with the same experiment scheme. The ship-borne test platform is composed of SINS, DVL and GPS receiver. The specifications of SINS and DVL are listed in Table 3 and Table 4. The update interval is 0.005 s and the total test time is 10 000 s. The integrated SINS/GPS provides the reference of high accuracy for SINS/DVL. The test trajectory is shown in Fig. 6.

Table 3 Specifications of SINS

Quantity	Gyro	Accelerometer
Dynamic range	±400°/s	±10g
Bias	⩽0.003°/h	⩽5 mg
Update rate	200 Hz	200 Hz

Table 4 Specifications of DVL

Quantity	DVL
Speed range/kn	−10 to 10
Bias/(cm/s)	0.3%±0.3
Update rate/Hz	1
Depth of the botton track/m	80

Fig. 6 Trajectory of shipboard test

For the attitude estimation errors shown in Fig. 7–Fig. 9, it is obvious that the estimation performance of Dual-AUKF outperforms that of SH-AUKF and UKF. The pitch error and roll error of Dual-AUKF are obviously less than SH-AUKF and UKF. The attitude changes of ships are different from those of vehicles, and the movement attitude of ships is relatively obvious. For the yaw estimation error shown in Fig. 9, Dual-AUKF is not always smaller than SH-AUKF and UKF, but it is the most stable of the three methods, always smaller than 0.03° after 4 000 s.

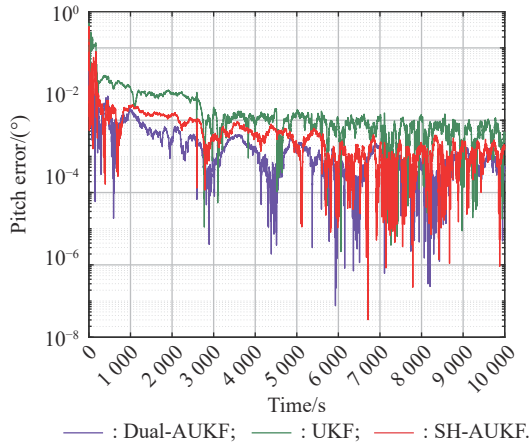

Fig. 7 Pitch estimate errors

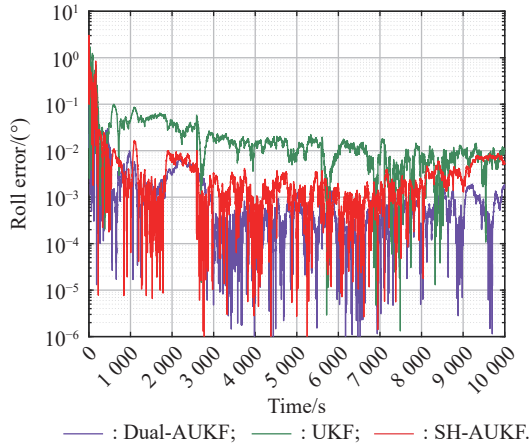

Fig. 8 Roll estimate errors

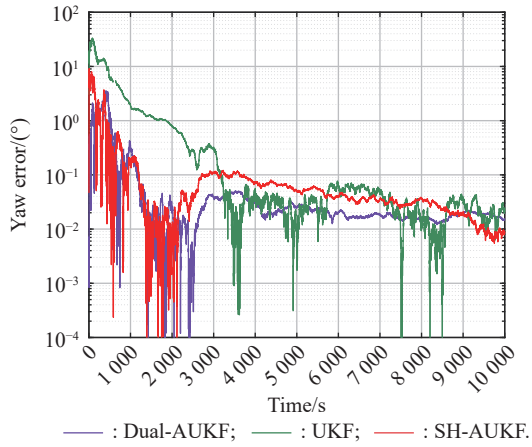

Fig. 9 Yaw estimate errors

The accuracy of the position obtained by three methods are also examined in Fig. 10 and Fig. 11. The average of position errors of three methods are (113.733 3 m, 136.197 4 m), (39.744 8 m, 22.574 2 m), (29.525 9 m, 24.562 7 m), respectively. Compared with SH-AUKF, the

latitude error and longitude error decline by 25.7% and 8.8%, respectively. Obviously, Dual-AUKF has strong robustness and stability.

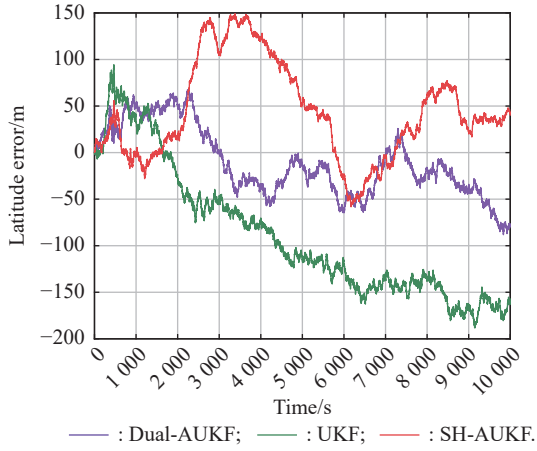

Fig. 10 Latitude estimate errors

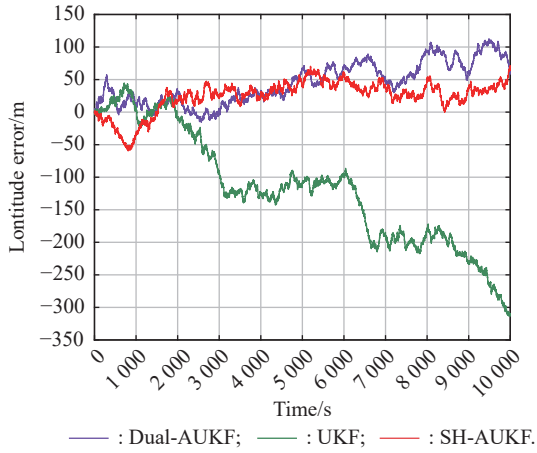

Fig. 11 Longitude estimate errors

5. Conclusions

An integrated navigation method based on Dual-AKFs is proposed in this paper. The measurement noise matrix is obtained by estimating the diagonal terms of the covariance matrix of the measurement noise error vector. It is found that this method has better performance than the SH-AKF when the noise covariance is unknown or non-Gaussian in integrated navigation. The performance of Dual-AUKF has been significantly improved, and the adaptability of the method has been enhanced. It is tested in vehicle-mounted and ship-mounted integrated navigation systems, and the superiority of this method in navigation accuracy and consistency is effectively verified.

References

[1] LYU X, HU B Q, DAI Y B, et al. Gaussian process regression-based quaternion unscented Kalman robust filter for integrated SINS/GNSS. Journal of Systems Engineering and Electronics, 2022, 33(5): 1079–1088.

[2] LI K L, LU X, LI W K. Nonlinear error model based on quaternion for the INS: analysis and comparison. IEEE Trans. on Vehicular Technology, 2020, 70(1): 263–272.

[3] CHANG L, NIU X J, LIU T Y. GNSS/IMU/ODO/LiDAR-SLAM integrated navigation system using IMU/ODO pre-integration. Sensors, 2020, 20(17): 4702.

[4] LYU X, HU B Q, WANG Z, et al. A SINS/GNSS/VDM integrated navigation fault-tolerant mechanism based on adaptive information sharing factor. IEEE Trans. on Instrumentation and Measurement, 2022, 71: 9506913.

[5] WANG D, XU X S, YAO Y Q, et al. A novel SINS/DVL tightly integrated navigation method for complex environment. IEEE Trans. on Instrumentation and Measurement, 2019, 69(7): 5183–5196.

[6] FENG K Q, LI J, ZHANG X, et al. An improved strong tracking cubature Kalman filter for GPS/INS integrated navigation systems. Sensors, 2018, 18(6): 1919.

[7] LI K L, HU B Q, CHANG L B, et al. Comparison of direct navigation mode and indirect navigation mode for integrated SINS/GPS. Transactions of the Institute of Measurement and Control, 2016, 38(1): 3–13.

[8] CHANG L B, LI J S, CHENG S Y. Initial alignment by attitude estimation for strapdown inertial navigation systems. IEEE Trans. on Instrumentation and Measurement, 2014, 64(3): 784–794.

[9] KARAMAT T B, LINS R G, GIVIGI S N, et al, Novel EKF-based vision/inertial system integration for improved navigation. IEEE Trans. on Instrumentation and Measurement, 2018, 67(1): 116−125.

[10] ZHU T G, LI A, LI K L, et al. The quaternion based error model based on SE(3) of the INS. IEEE Sensors Journal, 2022, 22(13): 13067–13077.

[11] LI K L, CHANG L B, HU B Q. A variational Bayesian-based unscented Kalman filter with both adaptivity and robustness. IEEE Sensors Journal, 2016, 16(18): 6966–6976.

[12] LYU X, HU B Q, LI K L, et al. An adaptive and robust UKF approach based on gaussian process regression-aided variational bayesian. IEEE Sensors Journal, 2021, 21(7): 9500–9514.

[13] GAO D Y, HU B Q, CHANG L B, et al. An aided navigation method based on strapdown gravity gradiometer. Sensors, 2021, 21(3): 829.

[14] NARSIMHAPPA M, MAHINDRAKAR A D, et al. An improved Sage Husa adaptive robust Kalman filter for denoising the MEMS IMU drift signal. Proc. of the IEEE Indian Control Conference, 2018: 229−234.

[15] MEHRA R. On the identification of variances and adaptive Kalman filtering. IEEE Trans. on Automatic Control, 1970, 15(2): 175–184.

[16] SUN J R, TAO L, NIU Z, et al. An improved adaptive unscented kalman filter with application in the deeply integrated BDS/INS navigation system. IEEE Access, 2020, 8: 95321–95332.

[17] XU Y L, LIU W Q, DING X Q, et al. USBL positioning system based adaptive kalman filter in AUV. Proc. of the OCEANS-MTS/IEEE Kobe Techno-Oceans Conference, 2018: 28−31.

[18] HOU L H, XU X S, YAO Y Q, et al. Improved exponential weighted moving average based measurement noise estimation for strapdown inertial navigation system/ Doppler velo-

city log integrated system. The Journal of Navigation, 2021, 74(2): 467–487.
[19] MENG Y, GAO S S, ZHONG Y M, et al. Covariance matching based adaptive unscented Kalman filter for direct filtering in INS/GNSS integration. Acta Astronautica, 2016, 120(3): 171–181.
[20] ASROZA R, ALESSANDRI A, CONTE J P. A dual adaptive filtering approach for nonlinear finite element model updating accounting for modeling uncertainty. Mechanical Systems and Signal Processing, 2019, 115: 782–800.
[21] SONG M, ASTROZA R, EBRAHIMIAN H, et al. Adaptive Kalman filters for nonlinear finite element model updating. Mechanical Systems and Signal Processing, 2020, 143: 106837.
[22] GUO F, HU G D, XIANG S, et al. A multi-scale parameter adaptive method for state of charge and parameter estimation of lithium-ion batteries using dual Kalman filters. Energy, 2019, 178(7): 79–88.
[23] LI J B, YE M, GAO K P, et al. Joint estimation of state of charge and state of health for lithium-ion battery based on dual adaptive extended Kalman filter. International Journal of Energy Research, 2021, 45(9): 13307–13322.
[24] JULIER S J, UHLMAN J K. Unscented filtering and nonlinear estimation. Proceedings of the IEEE, 2004, 92(3): 401–422.

Biographies

LYU Xu was born in 1990. He received his B.S. and M.S. degrees in control theory and control engineering from the Department of Electrical Engineering, Liaoning University of Technology, Jinzhou, China, in 2014 and 2019, respectively, and Ph.D. degree in navigation, guidance, and control from the Department of Navigation Engineering, Naval University of Engineering, Wuhan, China, in 2022. He is currently a postdoctoral fellow with the Department of Precision Instrument, Tsinghua University, Beijing, China. His main research interests include inertial navigation systems, integrated navigation, and predictive control.
E-mail: lvlay@163.com

MENG Ziyang was born in 1984. He received his B.S. degree from Huazhong University of Science and Technology, Wuhan, China in 2006, and Ph.D. degree from Tsinghua University, Beijing, China, in 2010. He was an Exchange Ph.D. student with Utah State University, Logan, UT, USA, from 2008 to 2009. He is currently an associate professor with the Department of Precision Instrument, Tsinghua University. Prior to joining Tsinghua University, he was a post doctoral researcher, a researcher, and a humboldt research fellow with Shanghai Jiao Tong University, Shanghai, China, the KTH Royal Institute of Technology, Stockholm, Sweden, and the Technical University of Munich, Munich, Germany, respectively, from 2010 to 2015. His research interests include distributed control and optimization and intelligent navigation technique.
E-mail: ziyangmeng@tsinghua.edu.cn

LI Chunyu was born in 1992. He received his B.S. degree in vehicle engineering from Hunan University, Changsha, China, in 2015, M.S. degree in automotive engineering from University of Bath, Bath, U.K., in 2016, and Ph.D. degree in aeronautical and astronautical science and technology from Beijing Institute of Technology, Beijing, China, in 2023. He is currently a post-doctoral researcher with the Department of Precision Instrument, Tsinghua University, Beijing, China. His main research interests include distributed state estimation and visual-inertial navigation systems.
E-mail: lcyfly1@163.com

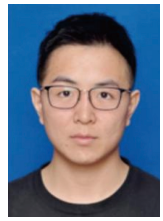

CAI Zhenyu was born in 1998. He received his B.S. degree in engineering from the School of Mechanical Engineering, Wuhan Polytechnic University in 2020. Currently he is studying for his M.S. degree in the School of Mechanical and Power School, the China Three Gorges University. His research interests include inertial navigation and motion attitude control.
E-mail: 592178236@qq.com

HUANG Yi was born in 1985. He received his B.S. degree in remote sensing information from the Information Engineering University in 2007, M.S. degree in geographic information systems from China University of Petroleum (Beijing) in 2018. He is now an engineer with Unit 91001 of the PLA. His research interests include geographic information systems and ship navigation.
E-mail: lx_bird@126.com

LI Xiaoyong was born in 1997. He received his B.S. degree in surveying and mapping engineering from Wuhan University, Wuhan, China, in 2020, M.S. degree in control engineering and electronic information from Naval University of Engineering, Wuhan, China, in 2022. He is now an engineer with Unit 91001 of the PLA. His main research interests include geographic information systems and ship navigation.
E-mail: 2016301610349@whu.edu.cn

YU Xingkai was born in 1988. He received his Ph.D. degree in control science and engineering from Shanghai Jiao Tong University in 2019. From 2019 to 2022, he was a post-doctoral fellow with the Department of Precision Instrument, Tsinghua University, Beijing, China. He is currently a distinguished associate professor with the School of Control and Computer Engineering, North China Electric Power University, Beijing, China. His main research interests include distributed state estimation, information fusion, system identification, and their applications in navigation technology and target tracking.
E-mail: yuxingkai2007@163.com